strates with one thymidine adjacent to the oligonucleotide binding site should afford cleavage of a single bond.

Termination of the cleavage reaction at short reaction times resulted in highly selective hydrolysis, whereas longer reaction times caused an increasing amount of nonselective secondary cleavage of the substrate DNA. Nonselective cleavage may arise from autocleavage of the oligonucleotide binding domain, a problem that may be overcome with a nonhydrolyzable binding site. Cleavage of the substrate without prior hybridization also resulted in selective cleavage, suggesting that nonselective cleavage by the hybrid enzyme is slow. The addition of 1 μg of poly(dA) DNA to the reaction mixture decreased nonselective cleavage of the substrate DNA. In conclusion, we have demonstrated that selective introduction of an oligonucleotide binding site into the relatively nonselective DNase staphylococcal nuclease generates a hybrid sequence-specific DNase. It may be possible to rationally alter the specificity of other enzymes by a similar strategy.

REFERENCES AND NOTES

1. D. A. Estell *et al.*, *Science* **223**, 659 (1986); C. N. Cronin, B. A. Malcolm, J. F. Kirsch, *J. Am. Chem. Soc.* **109**, 2222 (1987).
2. A. Podhajska and W. Szybalski, *Gene* **40**, 175 (1985).
3. G. B. Dreyer and P. B. Dervan, *Proc. Natl. Acad. Sci. U.S.A.* **82**, 968 (1985).
4. B. C. Chu and L. E. Orgel, *ibid.*, p. 963.
5. V. V. Vlassov, V. F. Zarytova, I. V. Kutiaven, S. V. Mamaev, M. A. Podyminogin, *Nucleic Acids Res.* **14**, 4065 (1986); B. L. Iverson and P. B. Dervan, *J. Am. Chem. Soc.* **109**, 1241 (1987).
6. P. Cuatrecasas, S. Fuchs, C. Anfinsen, *J. Biol. Chem.* **242**, 1541 (1967).
7. P. W. Tucker, F. Cotton, E. Hazen, *Mol. Cell Biochem.* **22**, 67 (1978); *ibid.* **23**, 3 (1979).
8. ———, *ibid.*, p. 67.
9. I. Chaiken and G. R. Sanchez, *J. Biol. Chem.* **247**, 6743 (1972).
10. L. Cunningham, *J. Am. Chem. Soc.* **80**, 2546 (1958); A. Mikulski, E. Sulkowski, L. Stasink, M. Laskowski, *J. Biol. Chem.* **244**, 6559 (1969); W. Hörz and W. Altenburger, *Nucleic Acids Res.* **9**, 2643 (1981).
11. F. A. Cotton, E. E. Hazen, M. J. Legg, *Proc. Natl. Acad. Sci. U.S.A.* **76**, 2551 (1979).
12. E. H. Serpersu, D. Shortle, A. S. Mildvan, *Biochemistry* **26**, 1289 (1987).
13. Calculated with the program by S. Lipson and U. C. Berkeley, which is based on work by K. J. Breslauer, R. Frank, H. Blocker and L. A. Markey [*Proc. Natl. Acad. Sci. U.S.A.* **83**, 3746 (1986)].
14. R. Zuckermann, D. Corey, P. G. Schultz, *Nucleic Acids Res.* **15**, 4403 (1987).
15. H. Taniuchi and C. B. Anfinsen, *J. Biol. Chem.* **241**, 4366 (1966).
16. D. Shortle, *Gene* (1983), p. 181.
17. M. Takahara, D. W. Hibler, P. J. Barr, J. A. Gerlt, M. Inouye, *J. Biol. Chem.* **260**, 2670 (1985).
18. The Hind III–Sal I fragment of the plasmid pONF 1, which encodes residues 102 to 149 of the nuclease gene, was inserted into the polylinker site of M13mp18. Single-stranded DNA that contained misincorporated uracil was then produced by the method of Kunkel with *Escherichia coli* RZ 1032 (*19*). The mutagenesis primer 5′-ATGTTTACTGCCCTAACAAT-3′ was annealed to the template DNA and mutagenesis was performed by the method of Zoller and Smith (*20*). Mutant sequences were confirmed by Sanger sequencing (*21*) of the entire insert, and the mutant sequence was reinserted into plasmid pONF 1 to reconstruct the gene that encodes the Cys^{116} mutant enzyme. The Cys^{116} mutant nuclease was purified from *E. coli* DH 1. The transformed cells were grown to midlog phase and induced by the addition of lactose (2 m*M* final concentration). The enzyme was purified by the method of Shortle (*22*) and dialyzed against 50 m*M* NaCl, 2 m*M* Hepes, *p*H 6.8, to afford 15 mg (*23*) of purified enzyme from 20 g of cells.
19. T. A. Kunkel, *Proc. Natl. Acad. Sci. U.S.A.* **82**, 488 (1985).
20. M. Zoller and M. Smith, *Methods Enzymol.* **100**, 468 (1983).
21. F. Sanger, S. Nicklen, A. R. Coulson, *Proc. Natl. Acad. Sci. U.S.A.* **24**, 5463 (1977).
22. D. Shortle, *J. Cell. Biochem.* **30**, 125 (1986).
23. Protein concentration was determined by absorbance at 280 nm: $\epsilon_{1\text{ cm}}^{0.1\%} = 0.93$ at neutral *p*H (*5*).
24. U. Laemmli, *Nature (London)* **227**, 680 (1970).
25. Thiols were titrated with 5,5′-dithiobis(2-nitrobenzoate) in 0.050*M* NaCl, 0.002*M* Hepes, *p*H 6.8. No thiols were detected in the dimeric enzyme.
26. T. Maniatis, E. F. Fritsch, J. Sambrook, *Molecular Cloning: A Laboratory Manual* (Cold Spring Harbor Laboratory, Cold Spring Harbor, NY, 1982), p. 122
27. A. M. Maxam and W. Gilbert, *Proc. Natl. Acad. Sci. U.S.A.* **74**, 560 (1977).
28. Determined by densitometry of the gel autoradiograms (Fig. 4).

29. Supported in part by a Presidential Young Investigator Award from the National Science Foundation (CHE85-43106) and by the Petroleum Research Foundation, administered by the American Chemical Society. We thank J. Gerlt for the gift of plasmid pONF 1.

19 June 1987; accepted 23 October 1987

A Complete Mapping of the Proteins in the Small Ribosomal Subunit of *Escherichia coli*

M. S. CAPEL, D. M. ENGELMAN, B. R. FREEBORN, M. KJELDGAARD,* J. A. LANGER,† V. RAMAKRISHNAN, D. G. SCHINDLER,‡ D. K. SCHNEIDER, B. P. SCHOENBORN, I.-Y. SILLERS,§ S. YABUKI,‖ P. B. Moore

The relative positions of the centers of mass of the 21 proteins of the 30*S* ribosomal subunit from *Escherichia coli* have been determined by triangulation using neutron scattering data. The resulting map of the quaternary structure of the small ribosomal subunit is presented, and comparisons are made with structural data from other sources.

THE POLYMERIZATION OF AMINO ACids to form proteins is catalyzed in all organisms by a nucleoprotein enzyme known as the ribosome. Ribosomes are template-directed polymerases whose substrates are aminoacyl–transfer RNAs; messenger RNAs are their templates.

The ribosome of *Escherichia coli* is a typical prokaryotic ribosome, similar in design to its larger, eukaryotic homologs (*1*). It consists of a large, 50*S* subunit and a small, 30*S* subunit. The 50*S* subunit contains 32 different proteins (average molecular weight ~14,500) and two ribosomal RNAs (rRNAs), 5*S* RNA (120 nucleotides) and 23*S* RNA (2904 nucleotides). The 30*S* subunit has 21 proteins (average molecular weight ~16,500) and a single 16*S* rRNA (1541 nucleotides). The proteins of both ribosomal subunits are present in unit stoichiometry with the exception of the 50*S* protein L7-L12, which is present as a tetramer (L7 is an acetylated form of L12) (*2*). The molecular weight of the assembly is 2.3×10^6, exclusive of counterions.

The overall structure of the *E. coli* ribosome has been investigated by image reconstruction methods at low resolution [for example (*3*)], and an atomic resolution, crystallographic structure may ultimately become available (*4*). A large number of methods have been used to probe its quaternary organization: immune–electron microscopy (IEM) (*5, 6*), chemical cross-linking (*7, 8*), fluorescence energy transfer (FET) (*9*), and neutron scattering (*10–12*). Assembly of the ribosome (*13*) and the protein binding sites on the rRNAs (*14*) have also been studied. The completed analysis of the positions of the proteins in the small ribosomal subunit of *E. coli* by neutron scattering is presented here.

M. S. Capel, V. Ramakrishnan, D. K. Schneider, B. P. Schoenborn, Biology Department, Brookhaven National Laboratory, Upton, NY 11973.
D. M. Engelman, J. A. Langer, D. G. Schindler, Department of Molecular Biophysics and Biochemistry, Yale University, New Haven, CT 06511.
B. R. Freeborn, M. Kjeldgaard, I.-Y. Sillers, S. Yabuki, P. B. Moore, Department of Chemistry, Yale University, New Haven, CT 06511.

*Present address: Division of Biostructural Chemistry, Kemisk Institut, Aarhus Universitet, DK-8000 Aarhus C, Denmark.
†Present address: Department of Molecular Genetics and Microbiology, UMDNJ–Robert Wood Johnson Medical School, 675 Hoes Lane, Piscataway, NJ 08854.
‡Present address: Department of Chemical Immunology, Weizmann Institute of Science, Rehovot 76100, Israel.
§Present address: 3402 Cummings Lane, Chevy Chase, MD 20815.
‖Present address: Department of Physics, Faculty of General Studies, Gunma University, 4-2 Aramaki-machi, Maebashi 371, Japan.

The strategy and techniques necessary for neutron-distance mapping have been discussed in detail (*15–17*). Each experiment measures the contribution made to the neutron scattering profile of a structure by the interference between the scattering of a pair of its components. The magnitude of that contribution can be varied by reconstituting 16*S* rRNA and a mixture of purified 30*S* proteins, one or more of which is labeled with deuterium in nonexchangeable positions.

Each interpretation distance measurement requires the preparation of four reconstituted 30*S* particles: (i) preparation A, a 30*S* particle in which both proteins of interest are labeled, (ii) preparation B, a 30*S* particle in which none of the proteins are labeled, (iii) preparation C, subunits in which one of the proteins of interest is labeled, and (iv) preparation D, subunits in which the other member of the pair is labeled. For those pairs of proteins that bind irreversibly to the 30*S* subunit, reconstituted preparations A and B are mixed in equimolar proportion as are preparations C and D, and the solution scattering profiles of both mixtures are measured. The pair interference profile, $I_X(s)$, is the difference of the scattering profiles of the two mixtures:

$$I_X(s) = I_{A,B}(s) - I_{C,D}(s), \qquad (1)$$

where s is the equivalent Bragg spacing [$s = 2\sin(\theta/\lambda)$], θ is half the scattering angle, and λ is the wavelength of the neutrons being used (*17*). (Equation 1 holds exactly if the amounts of ribosomal material in the two mixed samples are equal. If they are not, corrections for contributions due to buffer scattering and other factors must be taken into account.)

When one or both members of the pair bind reversibly to the 30*S* subunit, the scattering profiles of all four reconstituted particles are measured separately, and the pair interference profile is calculated from the appropriately scaled and corrected scattering profiles (*15*):

$$I_X(s) = I_A(s) + I_B(s) - I_C(s) - I_D(s) \quad (2)$$

However it is obtained, $I_X(s)$ reflects the spatial relationship of the pair of components in question, an important aspect of which is the distance between their centers of mass (centroids).

The Fourier transform of $I_X(s)$, $p(r)$, is the distribution of lengths of all possible vectors connecting nonexchangeable hydrogen sites in the two proteins whose isotopic compositions were varied in the experiment. The second moment of the length distribution related to a pair of proteins is equal to the sum of squares of their radii of gyration (in situ) plus the square of the separation between their centroids (*18*).

As long as there are more than eight components in an assembly, there will be more second moments available than there are component coordinates and radii of gyration to be specified. Estimates for coordinates and radii of gyration can be extracted from a set of second moment data by nonlinear optimization techniques (*19*). The second moments from 105 distances data sets relating 93 different protein pairs in the 30*S* subunit are now available, appreciably more than the minimum of 78 required for a

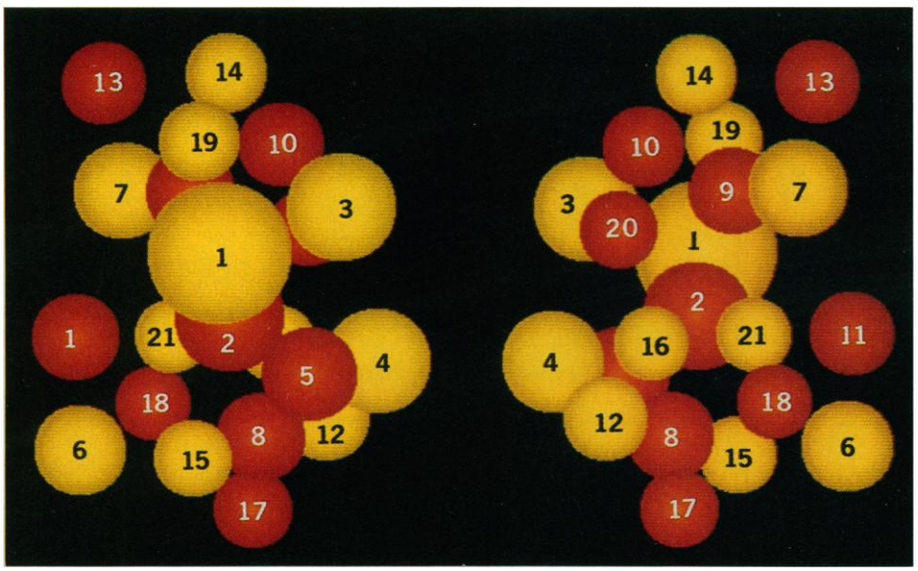

Fig. 1. Two views of the neutron map of the 30*S* ribosomal subunit from *E. coli*. Each protein is represented by a sphere whose volume is the same as that of the protein. The centers of the spheres are at the positions given in Table 1. The maximum linear dimension of the array is about 190 Å. Coloring of the spheres is intended as an aid to depth perception. Numbering of the proteins adheres to the standard nomenclature for ribosomal proteins (*2*). The two views are related to each other by a 180° rotation about an axis oriented vertically in the plane of the figure.

Table 1. Positions and radii of gyration of proteins in the 30*S* ribosomal subunit. Coordinates of the centroids of the proteins (x, y, z) in the 30*S* subunit, their radii of gyration (Rg), and standard error estimates (σ) are provided. All values are given to the nearest 0.1 Å. The origin of the coordinate system is the center of S3. The x axis is the S3 to S4 direction. The y axis is the component of the S3 to S5 vector normal to the S3 to S4 direction. The z axis is the component of the S3 to S8 vector normal to both of the other axes.

Protein	x	σ_x	y	σ_y	z	σ_z	Rg	σ_{Rg}
S1	0.7	12.2	54.9	16.7	8.0	16.5	55.4	13.5
S2	24.8	8.0	53.4	7.8	14.7	10.0	32.8	7.3
S3	0.	0.	0.	0.	0.	0.	25.4	8.0
S4	58.1	2.8	0.	0.	0.	0.	30.2	4.6
S5	53.0	5.0	39.3	3.4	0.	0.	13.5*	7.8
S6	58.7	14.5	64.3	11.8	93.9	6.4	13.1*	1.0
S7	−28.6	9.8	28.7	9.0	67.4	9.6	13.7*	1.8
S8	70.9	7.6	50.9	6.1	21.6	5.1	21.1	3.9
S9	−22.1	7.3	26.6	6.9	39.5	8.5	20.8	2.6
S10	−27.3	4.3	−5.4	7.9	19.4	7.6	12.6	5.6
S11	15.5	13.2	85.8	7.3	62.4	10.6	12.5*	0.9
S12	74.7	5.3	−1.6	7.4	36.7	5.2	12.6*	1.4
S13	−71.4	9.0	51.1	12.2	42.6	17.7	12.5*	2.7
S14	−60.2	6.4	24.1	13.8	6.0	12.8	12.0	4.2
S15	68.0	13.6	82.3	5.7	28.0	9.2	26.8*	1.3
S16	42.5	5.9	9.5	9.5	39.4	9.3	25.7	12.3
S17	97.8	10.2	40.7	10.8	45.8	6.7	13.2	20.4
S18	51.2	17.1	36.3	11.0	78.5	5.4	10.9*	1.0
S19	−41.7	9.9	54.7	11.4	1.5	14.1	11.6*	2.4
S20	6.7	4.6	−20.7	5.4	33.0	8.1	11.3*	2.2
S21	27.9	11.0	41.8	10.0	55.6	7.1	24.8*	1.3

*Values determined by contraints imposed during construction of the map. In most cases the active constraint requires that no protein have a radius of gyration smaller than a sphere of equivalent volume. For S15 and S21 the constraint is that radii may not exceed 2.5 to 3 times the minimum sphere value. The errors assigned constrained radii are small due to the action of the constraints; they are not true indicators of the quality of the data.

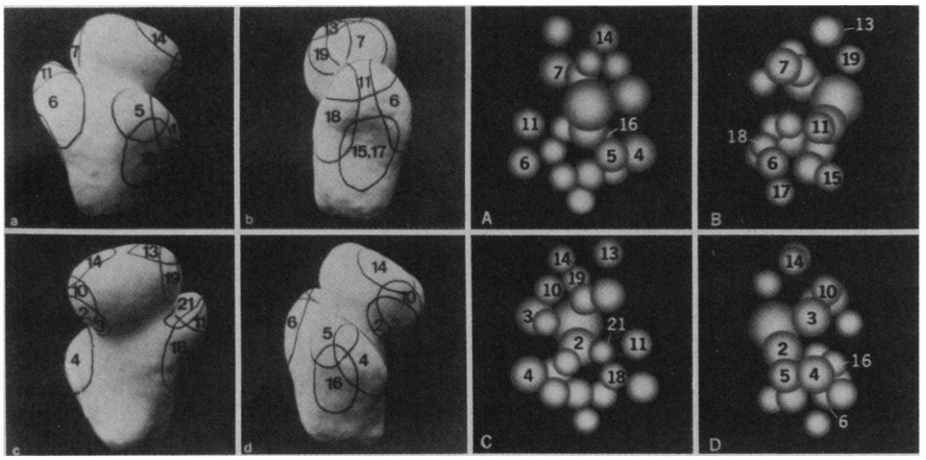

Fig. 2. Comparison of an IEM map (*5*) with the neutron map. Four views of the shape of the 30*S* ribosomal subunit are shown in the left-hand pictures with locations for antigenic determinants as determined by electron microscopy (*5*). The right-hand block contains four views of the neutron map in roughy corresponding orientations. The images in the two rows are not scaled to the same size.

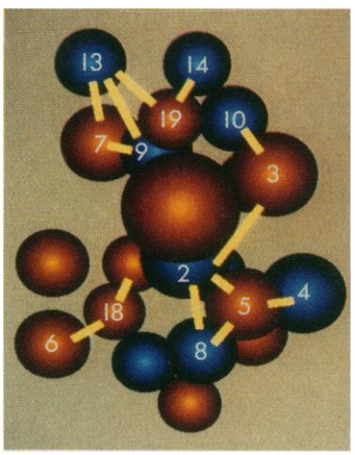

Fig. 3. Cross-linking relationships. The protein-protein cross-links that have been reported by two or more independent groups are represented as bars connecting the proteins (*8*).

21-protein structure. Seventy-one of these data sets have been presented elsewhere (*12*); the remaining 34 are in preparation (*20*). Of the 34 unpublished data sets, 12 have been obtained since the last partial mapping of the subunit (*11*).

It is a characteristic of distance mapping that as the data accumulate, more complete partial maps can be calculated with greater accuracy (*11, 12*). Each second moment added to the data set affects the mapping of all components, not just the pair whose separation is estimated by that second moment (*19*). So that the convergence of the neutron map to a final model can be assessed, the coordinates for all components must be examined in each map, not just the coordinates of components located by the new data. For this reason, the centroid coordinates and radii of gyration for all proteins in the 30*S* subunit are presented in Table 1. Two views of the model for the distribution of proteins in the small ribosomal subunit are shown in Fig. 1.

A fundamental limitation of distance mapping is that it cannot distinguish between structures that are enantiomers. The enantiomer presented here has been shown to be the correct one by electron microscopy (*21*).

The proteins of the 30*S* subunit are small relative to their average separations. The second moments are dominated by the separations between proteins. The result is that coordinates are better determined than radii of gyration in this map, which is apparent from the standard error estimates in Table 1. The data on radii of gyration argue that proteins S1, S2, and S4 have large axial ratios but do not permit firm conclusions to be drawn about the others, many of which appear to have small axial ratios.

Two groups have mapped the antigenic determinants of individual ribosomal proteins relative to topographical features of the surface of the 30*S* subunit by IEM methods (*5, 6*). The logical union of the two IEM maps provides reasonably consistent estimates for the positions of 18 of the 21 30*S* proteins. Four views of the IEM map of the Berlin group (*5*) are compared with four views of the neutron map in Fig. 2. (In Fig. 2 the IEM views are on a different scale from the neutron views.) It is clear that the clustering of antigenic determinants in the IEM map is similar to the clusterings of protein centers in the neutron map. The same is true of the UCLA map (*6*). The correlation is weakest for proteins S2, S16, and S19. Further work will be required to decide precisely where these proteins are in the structure.

The results of protein cross-linking experiments on the 30*S* subunit with bifunctional reagents (*8*) are compared with the neutron map in Fig. 3. All the cross-links between pairs of proteins that have been reported by two or more laboratories are represented by bars connecting the appropriate proteins. Cross-linking studies have led to the identification of a significant number of nearest neighbor relationships in this structure, but not all of them.

It is clear from these comparisons that the neutron map is consistent with other independent sources of information. Thus, there is reason to believe that the neutron map is a reasonable approximation to the true quaternary structure of the 30*S* ribosomal subunit. A complete statistical analysis of this map will appear elsewhere (*20*) as well as a description of the correlations that can be made between the structure shown here and its function (*22*).

REFERENCES AND NOTES

1. I. G. Wool, in *Structure, Function, and Genetics of Ribosomes*, B. Hardesty and G. Kramer, Eds. (Springer-Verlag, New York, 1986), p. 391.
2. L. Giri, W. E. Hill, H. G. Wittmann, B. Wittmann-Leibold, *Adv. Protein Chem.* **36**, 1 (1984); B. Wittmann-Liebold, in *Structure, Function, and Genetics of Ribosomes*, B. Hardesty and G. Kramer, Eds. (Springer-Verlag, New York, 1986), p. 326; H. F. Noller, *Annu. Rev. Biochem.* **53**, 119 (1984).
3. M. Rademacher, T. Wagenknecht, A. Verschoor, J. Frank, *J. Microsc.* **141**, PR1 (1986); A. Yonath, K. R. Leonard, H. G. Wittmann, *Science* **236**, 813 (1987).
4. A. Yonath, M. A. Saper, H. G. Wittmann, in *Structure, Function, and Genetics of Ribosomes*, B. Hardesty and G. Kramer, Eds. (Springer-Verlag, New York, 1986) p. 112; A. Yonath *et al.*, *52nd Cold Spring Harbor Symp. Quant. Biol.* (1987), abstracts, p. 24.
5. G. Stoeffler and M. Stoeffler-Meilicke, *Annu. Rev. Biophys. Bioeng.* **13**, 303 (1984); in *Structure, Function, and Genetics of Ribosomes*, B. Hardesty and G. Kramer, Eds. (Springer-Verlag, New York, 1986), p. 28.
6. M. O. Oakes, E. Henderson, A. Scheinman, M. Clark, J. A. Lake, in *Structure, Function, and Genetics of Ribosomes*, B. Hardesty and G. Kramer, Eds. (Springer-Verlag, New York, 1986), p. 47.
7. R. Brimacombe, P. Maly, C. Zweib, *Prog. Nucleic Acid. Res. Mol. Biol.* **28**, 1 (1983).
8. J. M. Lambert, G. Boileau, J.-A. Cover, R. R. Traut, *Biochemistry* **22**, 3913 (1983).
9. K. H. Huang, R. H. Fairclough, C. R. Cantor, *J. Mol. Biol.* **97**, 443 (1975).
10. J. A. Langer, D. M. Engelman, P. B. Moore, *ibid.* **119**, 463 (1978); V. Ramakrishnan *et al.*, *ibid.* **153**, 739 (1981); V. Nowotny, R. P. May, K. H. Nierhaus, in *Structure, Function, and Genetics of Ribosomes*, B. Hardesty and G. Kramer, Eds. (Springer-Verlag, New York, 1986), p. 101.
11. P. B. Moore, M. Capel, M. Kjeldgaard, D. M. Engelman, in *Structure, Function, and Genetics of Ribosomes*, B. Hardesty and G. Kramer, Eds. (Springer-Verlag, New York, 1986), p. 87.
12. V. Ramakrishnan, M. Capel, M. Kjeldgaard, D. M. Engelman, P. B. Moore, *J. Mol. Biol.* **174**, 265 (1984).
13. W. A. Held, B. Ballon, S. Mizushima, M. Nomura, *J. Biol. Chem.* **249**, 3273 (1974).
14. R. Brimacombe, J. Atmadja, A. Kyriatsoulis, W. Stiege, in *Structure, Function, and Genetics of Ribosomes*, B. Hardesty and G. Kramer, Eds. (Springer-Verlag, New York, 1986), p. 184.
15. D. M. Engelman and P. B. Moore, *Proc. Natl. Acad. Sci. U.S.A.* **69**, 1997 (1972).
16. P. B. Moore and D. M. Engelman, *Methods Enzymol.* **59**, 629 (1979); P. B. Moore, *ibid.*, p. 639; D. M. Engelman, *ibid.*, p. 656.
17. W. Hoppe, *Isr. J. Chem.* **10**, 321 (1972); W.

Hoppe, *J. Mol. Biol.* **78**, 581 (1972).
18. P. B. Moore, J. A. Langer, J. A. Engelman, D. M. Engelman, *J. Appl. Cryst.* **11**, 479 (1978); R. May, thesis, Technical University, Munich (1978); P. Stockel *et al.*, *J. Appl. Cryst.* **12**, 176 (1979).
19. P. B. Moore, E. Weinstein, *J. Appl. Cryst.* **12**, 321 (1979); V. Ramakrishnan and P. B. Moore, *J. Mol. Biol.* **174**, 719 (1981).
20. M. S. Capel, M. Kjeldgaard, D. M. Engelman, P. B. Moore, *J. Mol. Biol.*, in press.
21. K. R. Leonard and J. A. Lake, *ibid.* **129**, 155 (1979).
22. P. B. Moore and M. S. Capel, *Annu. Rev. Biophys. Chem.*, in press.
23. We thank G. Sun for her able technical assistance, the Brookhaven National Laboratory, the Office of Health and Environmental Research of the Department of Energy, the Institut Laue-Langevin, and G. Stoeffler and M. Stoeffler-Meilicke for supplying us with the photographs in Fig. 2. Supported by the National Science Foundation and NIH AI-20466 (D.M.E. and P.M.B.) and NIH AI-09167 (P.B.M.).

15 May 1987; accepted 9 September 1987

Decreased TRH Receptor mRNA Activity Precedes Homologous Downregulation: Assay in Oocytes

YORAM ORON,* RICHARD E. STRAUB, PAULA TRAKTMAN, MARVIN C. GERSHENGORN

Ligand-induced decrease in cell-surface receptor number (homologous downregulation) is often due to rapid receptor internalization. Thyrotropin-releasing hormone (TRH), however, causes a slow downregulation of TRH receptors (TRH-Rs), with a half-time of approximately 12 hours, in GH_3 rat pituitary cells. The mechanism of TRH-R downregulation was studied by monitoring TRH-evoked depolarizing currents in *Xenopus* oocytes injected with GH_3 cell RNA as a bioassay for TRH-R messenger RNA (mRNA) activity. In GH_3 cells, TRH caused a rapid decrease in TRH-R mRNA activity to 15 percent of control within 3 hours. Because the half-life of TRH-R mRNA activity in control cells was approximately 3 hours, the rapid decrease in mRNA activity was not due to inhibition of mRNA synthesis alone and may represent a post-transcriptional effect.

MODULATION OF CELL-SURFACE receptor number is an important mechanism of cell regulation. The number of available receptors on the cell surface may be decreased by ligand occupancy (homologous downregulation) that in many instances is caused by rapid receptor internalization (*1*). Thyrotropin-releasing hormone (TRH) downregulates the number of TRH receptors (TRH-Rs) on anterior pituitary cells (*2, 3*). The molecular mechanism that mediates regulation of TRH-R number is unknown but does not appear to involve rapid receptor internalization (*4*). The intracellular messengers that mediate TRH stimulation of hormone secretion, which include 1,2-diacylglycerol, inositol 1,4,5-trisphosphate, and calcium ion [for review, see (*5*)], may mediate TRH-R regulation. GH_3 rat pituitary tumor cells are an excellent model for study of TRH-R regulation, and variant clones that have few, if any, TRH-Rs (*4*) are available.

In *Xenopus* oocytes, muscarinic agonists cause membrane electrical responses consisting mainly of depolarizing chloride currents [for review, see (*6*)]. Muscarinic agonist stimulation of chloride currents is mediated by an elevation of intracellular calcium caused by inositol 1,4,5-trisphosphate (*7, 8*). Hence, muscarinic responses in *Xenopus* oocytes and TRH responses in GH_3 cells appear to be mediated by identical mechanisms. We reasoned, therefore, that RNA from GH_3 cells containing messenger RNA (mRNA) for TRH-Rs could be injected into *Xenopus* oocytes and translated, and when the TRH-Rs are inserted into the surface membrane, they could be monitored as acquired responsiveness to TRH. Injected oocytes could be used as a bioassay of TRH-R mRNA activity to study the mechanism of TRH-induced receptor downregulation.

In oocytes injected with total cytosolic RNA from GH_3 cells (120 to 400 ng per oocyte) and maintained under voltage clamp, TRH caused a marked membrane electrical response. Control oocytes (uninjected) did not respond to TRH (42 oocytes from ten frogs) but did respond to acetylcholine (ACh) (*9, 10*). The response to TRH was often observed by 8 to 12 hours and was maximal 30 to 72 hours after RNA injection. A typical response to 1 μM TRH (Fig. 1A) consisted of a very large (range

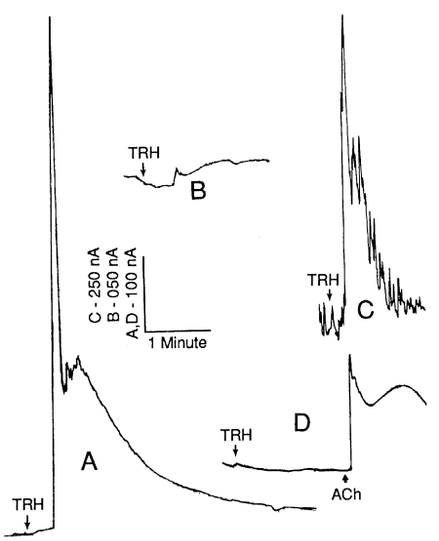

Fig. 1. Typical responses to TRH in *Xenopus* oocytes injected with RNA from GH_3 or GH-Y cells. (**A**) Oocyte injected with 320 ng of GH_3 cell RNA. (**B**) Oocyte injected with 20 ng of GH_3 cell RNA. (**C**) Oocyte injected with 20 ng of poly(A)$^+$ GH_3 cell RNA and 100 ng of carrier transfer RNA (*Escherichia coli*, Boehringer Mannheim). (**D**) Oocyte injected with 140 ng of RNA from GH-Y cells. Assays were performed 48 hours after injection. TRH (1 μM, light arrow) or 0.1 μM ACh (heavy arrow) was added for 1.5 minutes. For the preparation of oocytes, denuded oocytes were prepared as described by Dascal *et al.* (*12*). Oocytes were maintained at 20°C in 70% L-15 medium containing penicillin G (50 μg/ml) and 0.5 mM theophylline. For the preparation of total cytosolic RNA, cells were harvested with 0.02% EDTA, and washed three times with ice cold BSS (NaCl, 135 mM; KCl, 4.5 mM; glucose, 5.6 mM; $CaCl_2$, 1.5 mM; $MgCl_2$, 0.5 mM; and Hepes, 25 mM, *p*H 7.4). The cell pellet was resuspended in ten volumes of hypotonic lysis buffer (NaCl, 10 mM; $MgCl_2$, 1 mM; and tris-HCl, 10 mM, *p*H 7.4), kept on ice for 20 minutes, and vortexed three times for 1 minute at 5-minute intervals. After nuclei and debris were removed by centrifugation at 2000*g* for 10 minutes, the supernatant was diluted with four volumes of a solution containing 4M guanidinium thiocyanate, 0.5% *n*-lauroylsarcosine, 100 mM mercaptoethanol, and 25 mM sodium citrate, *p*H 7, layered onto a 3-ml cushion consisting of 5.7M CsCl and 100 mM EDTA, and centrifuged for 12 hours at 15°C in an SW41 rotor at 35,000 rpm. The RNA pellet was washed with cold 70% ethanol, dissolved in water, precipitated with ethanol, and again dissolved in water. Poly(A)$^+$-enriched RNA was purified by oligo(dT) affinity chromatography (*19*). For the intracellular injections, RNA (120 to 400 ng in 20 to 50 nl) was injected. Electrophysiological measurements were performed on oocytes that were voltage-clamped at −60 to −80 mV (*20*) as described (*10, 13*). In all experiments with GH_3 cell RNA, more than 90% of injected oocytes responded to TRH.

Y. Oron, R. E. Straub, M. C. Gershengorn, Division of Endocrinology and Metabolism, Department of Medicine, Cornell University Medical College, and New York Hospital, New York, NY 10021.
P. Traktman, Department of Cell Biology and Anatomy, Cornell University Medical College, New York, NY 10021.

*Permanent address: Department of Physiology and Pharmacology, Sackler Faculty of Medicine, Tel Aviv University, Ramat Aviv, Israel.